

Texture discrimination by an autonomous mobile brain-based device with whiskers

Anil K. Seth, Jeffrey L. McKinstry, Gerald M. Edelman, and Jeffrey L. Krichmar
The Neurosciences Institute, 10640 John Jay Hopkins Drive, San Diego, CA 92121

Abstract—Whiskers are widely used by many animal species for navigation and texture discrimination. This paper describes Darwin IX, a mobile physical device equipped with artificial whiskers, the behavior of which is controlled by a neural simulation based on the rat somatosensory system. During its autonomous behavior, Darwin IX is able to discriminate among textures in its environment and learns to avoid textures that are paired with aversive events.

I. INTRODUCTION

Haptic sensory information provided by mystacial vibrissae (whiskers) allows the rat to discriminate among different textures in its environment [8], [13]. Although whisker-based perception lacks the fine resolution and long range of vision, whiskers have the advantage of allowing navigation and discrimination in the dark. Previously, studies have focused on texture discrimination or contact localization by fixed whiskers or whisker arrays [6], [10], [14], or obstacle avoidance by mobile robots equipped with whiskers [3], [9].

To explore how haptic data may be used to discriminate among textures during autonomous behavior, we constructed Darwin IX, a mobile physical device equipped with artificial whiskers and a simulated nervous system based on the neuroanatomy of the rat somatosensory system. We show that neuronal units with time-lagged response properties, together with the selective modulation of neural connections strengths, provide a plausible neural mechanism for the spatiotemporal transformations of sensory input needed for both texture discrimination and selective conditioning to textures.

Darwin IX is the latest in a series of ‘brain-based devices’ (BBDs) that have been constructed over the last 12 years [5], [1], [11]. All BBDs in the Darwin series have the following attributes: 1) An embodied morphology that allows for active exploration in a real-world environment, including sensors such as proximity sensors and artificial whiskers. 2) A neural simulation to control the BBD’s behavior, incorporating detailed neuroanatomy and neurophysiology based on vertebrate nervous systems. 3) A value system that signals the salience of environmental cues and that modulates plasticity in the nervous system resulting in modification of the device’s behavior. These features result in a system that adapts its behavior via conditioning to become increasingly successful in coping with the environment.

In our experiments with Darwin IX, the device autonomously explored a walled environment containing two distinct textures each consisting of patterns of pegs embedded in the walls. It became conditioned to avoid one of the textures by

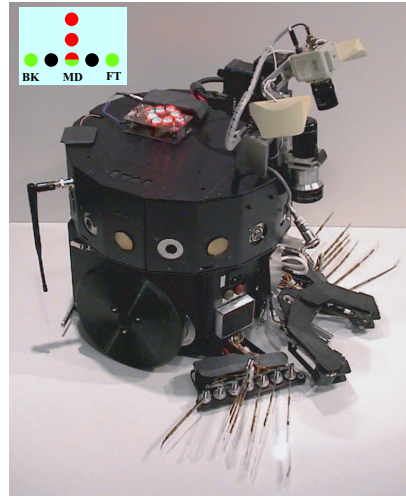


Fig. 1. Darwin IX consists of a mobile base equipped with several sensors and effectors including left and right whisker arrays, and a neural simulation running on a remote cluster of computer workstations. The arrangement of a whisker array is shown in the inset. Each array has 7 whiskers arranged in a row of 5 and a column of 3. Whiskers used for wall following are marked in green (FT,MD,BK). Whiskers that provide input to the neural simulation are marked in red. Note that one whisker (red/green) is used for both purposes. Whiskers marked in black are not used in the present model.

association of this texture with an innately aversive simulated ‘foot-shock’. Darwin IX demonstrated its conditioned behavior by freezing and then moving away from walls containing the texture corresponding to the aversive stimuli.

II. METHODS

Darwin IX consists of a mobile robotic base containing IR proximity sensors, custom-built whisker arrays, and a cluster of workstations that run the simulated nervous system and control the device’s behavior (Fig. 1). The cluster consists of six 1.4 GHz Pentium IV workstations running Message Passing Interface (MPI) parallel software under the Linux operating system. One workstation receives whisker and IR input information, and transmits motor commands, via an RF modem. A microcontroller (PIC17C756A) onboard the base samples input and status from the sensors and controls RS-232 communication between the robotic base and the workstations, via a wireless modem.

During each simulation cycle of Darwin IX, sensory input is processed, the state of the neural simulation is updated, and motor output is generated. In our experiments, execution of each cycle requires approximately 100ms of real time.

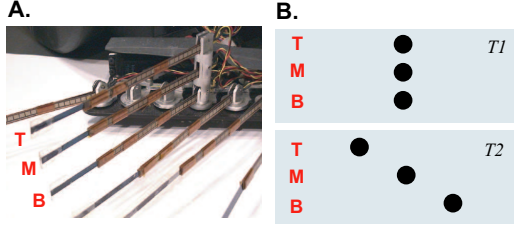


Fig. 2. **A.** Detail of a whisker array: The top (T), middle (M), and bottom (B) whiskers in the column are labeled; these whiskers provide input to the neural simulation. **B.** Schematic of textures $T1$ and $T2$. Each texture consists of pegs embedded in a wall; pegs are aligned in rows corresponding to the whiskers in a column. Pegs in the top row deflect the top whisker (T), and similarly for pegs in the middle row (M) and the bottom row (B).

A. Artificial whisker design

Each whisker array consists of seven whiskers arranged in a column of three and a row of five (see Fig. 1 (inset) and Fig. 2). Whisker columns supply input to the simulated nervous system, while whiskers in the rows support innate avoidance and wall following behaviors (see section *B. Innate behavior*). Each whisker consists of two 4cm by 0.63cm polyamide strips, adhered back-to-back, that are responsive to bend (Jameco, CA). These strips are typically used as strain sensors in devices such as virtual reality gloves. Each strip has 20 resistive areas embedded regularly along its length, providing a resistance of $\sim 10K\Omega$ when the strip is unbent and $\sim 50K\Omega$ when strip is maximally bent. Each strip detects bending in only one direction, hence the back-to-back arrangement. Voltage signals from each pair of strips (i.e. a whisker) are converted to a single signal ranging from 0V (maximum deflection in one direction) to 5V (maximum deflection in the opposite direction). These voltages are converted into digital signals, ranging from 0 to 256, by a 12-bit analog-to-digital converter at a sample rate of 40Hz. During each simulation cycle of Darwin IX a ‘packet’ of 4 signals for each whisker is received by the neural simulation. For whisker w_k at simulation cycle t , the corresponding packet is $[w_{k1}(t), w_{k2}(t), w_{k3}(t), w_{k4}(t)]$, where $w_{k4}(t)$ is the most recent. The first signal in each packet, $w_{k1}(t)$, which we call the ‘current whisker value’, is used for guiding Darwin IX’s wall following behavior; all four signals provide input to the neural simulation (see section *D. Whisker input and lag cells*).

B. Innate behavior

Darwin IX is equipped with innate behavioral responses. The default behavior of Darwin IX is to move forward in a straight line at a speed of $\sim 8\text{cm/sec}$. If Darwin IX approaches a wall head-on to within a distance of $\sim 4\text{cm}$, an avoidance response is triggered; the device stops, backs up ($\sim 10\text{cm}$), and then turns ~ 30 degrees away from the wall before resuming default behavior. Avoidance responses are triggered by two IR sensors, one facing front-left, and the other facing front-right.

Darwin IX has an innate freezing/escape response which is triggered by a simulated ‘foot-shock’, which is registered when a downward-facing IR sensor at the front of the device detects

TABLE I
WALL FOLLOWING BY DARWIN IX.

| Side | Whisker | φ_w | $g_w(wd(t) > 0)$ | $g_w(wd(t) \leq 0)$ |
|-------|---------|-------------|------------------|---------------------|
| Left | BK | 89 | 0.05 | 0.075 |
| | MD | 33 | 0.1 | 0.2 |
| Right | BK | 110 | 0.075 | 0.15 |
| | MD | 28 | 0.15 | 0.30 |

reflective construction paper (‘foot-shock pads’) on the floor of the arena. This response consists of continued movement for 55 simulation cycles ($\sim 5.5\text{s}$), freezing for 40 cycles ($\sim 4\text{s}$) then a turn away from the wall by an angle randomly chosen from the interval $[\pi/4, 3\pi/4]$.

Darwin IX also has an innate wall following capability such that, on encountering a wall, the device moves parallel to the wall at a distance suitable for the detection of embedded textures. Wall following is based on signals from the backmost (BK), the ‘middle’ whisker, which is lowest of the vertical stack (MD), and the frontmost (FT) on each side (see Fig. 1, inset). For each of these whiskers, a running average of the current whisker value (\bar{w}) is maintained over 75 simulation cycles. This average is updated at every cycle except when the current whisker value differs by more than 10 from the corresponding average (signifying whisker deflection; recall that the range of the current whisker value is 0-255). For each whisker on each side, a ‘deflection’ value wd is calculated as:

$$wd_{BK}(t) = |w_{BK1}(t) - \bar{w}_{BK}(t)| \quad (1)$$

$$wd_{MD}(t) = |w_{MD1}(t) - \bar{w}_{MD}(t)| \quad (2)$$

$$wd_{FT}(t) = |w_{FT1}(t) - \bar{w}_{FT}(t)| \quad (3)$$

Wall following of a left(right) wall is triggered when any deflection value for the left(right) whiskers exceeds 15. During each cycle of wall following, adjustments are made to the speed of the wheel furthest from the wall (the contralateral wheel); the other (ipsilateral) wheel remains at the default speed of $W_{def} = 35$. Contralateral wheel speeds are set using:

$$W_{speed} = W_{def} - back - mid - front \quad (4)$$

where $front = 0.25(wd_{FT})$, $mid = g_w(wd_{MD} - \varphi_w)$, and $back = g_w(wd_{BK} - \varphi_w)$, and where mid and $back$ are bounded in the range ± 5 , and g_w (a scaling factor) and φ_w (a threshold) are chosen according to the physical response characteristics of the whiskers (see Table I). Additionally, g_w varies according to the sign of the corresponding wd such that there is a bias in favor of turning towards a wall (see Table I, columns 4 and 5).

C. Neuroanatomy

Darwin IX’s simulated nervous system contains areas analogous to the somatosensory pathway in the rat brain, specifically the (ventromedial) nuclei of the thalamus, and primary and secondary somatosensory areas (in our model, $Th \rightarrow S1 \rightarrow S2$). Areas $S1$ and Th are subdivided into left (L) and right (R) regions and further into ‘top’ (T), ‘middle’ (M) and ‘bottom’

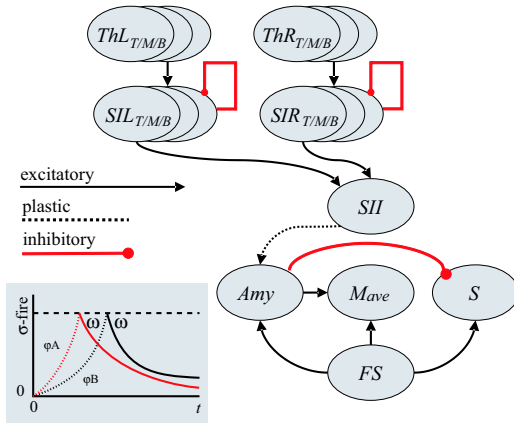


Fig. 3. Global neuroanatomy of Darwin IX. See text for details. **Inset.** The operation of two idealized lag cells (A and B). The post-stimulus internal state of cell A (s_A^{in}) rises quickly (red dashed line), at a rate determined by φ_A . The internal state of B (s_B^{in}) rises more slowly (black dashed line, φ_B). When the internal state of each cell reaches a threshold (σ^{fire}), output is generated (solid lines) which decays at a rate determined by ω .

(B) subregions, such that each subregion receives input from a single whisker in the column on the corresponding side.

A global diagram of Darwin IX’s simulated nervous system is given in Fig. 3. It comprises 17 areas, 1101 neuronal units (see Table II), and ~ 8400 synaptic connections (see Table III). Neuronal units in area *Th* respond to whisker input with unit-specific time delays (see section D. *Whisker input and lag cells*). These units project topographically to the corresponding units of *S1*. Each subregion of *S1* has local inhibitory connections which serve to increase the activity contrast among neuronal units. All subregions in *S1* project to area *S2* such that each neuronal unit in *S2* takes input from 3 neuronal units, each of which is in a different subregion of either the left sub-area or the right sub-area of *S1*. This arrangement ensures that synaptic input to a neuronal unit in *S2* is sparse and balanced. A deflection of a particular sequence of Darwin IX’s whiskers leads to a spatiotemporal pattern of activity in *S2*. Such a dynamic sequence is comparable to that observed in the rat brain [7].

Darwin IX’s nervous system also contains areas supporting the acquisition of conditioned aversion (see section G. *Aversive conditioning*). Area *FS* is activated by detection of a ‘foot-shock’ (see section H. *Experimental environment and protocol*), and projects to areas *Amy*, *Mave* and *S*. Area *Amy* is analogous to the amygdala, a neural area which has been widely implicated in the acquisition of conditioned fear [12]. Area *Mave* is analogous to a motor cortical area, activity in which elicits an innate aversive freezing/escape response.

Activity in the simulated value system, area *S*, signals the occurrence of salient sensory events and this activity contributes to the modulation of plastic connection strengths in the pathways $S2 \rightarrow Amy$. Initially, *S* is activated by detection of simulated ‘foot-shock’. Activity in *S* is analogous to that

TABLE II
NEURONAL UNIT PARAMETERS FOR DARWIN IX.

| Area | Size | σ^{fire} | ω | g |
|---------------|-------|-----------------|----------|------|
| <i>Th</i> (6) | 1x20 | 0.3 | 0.8 | - |
| <i>S1</i> (6) | 1x20 | 0.1 | 0.0 | 1.0 |
| <i>S2</i> | 30x30 | 0.2 | 0.8 | 1.0 |
| <i>S</i> | 1x1 | -0.10 | 0.0 | 1.0 |
| <i>Amy</i> | 1x1 | 0.0 | 0.0 | 1.75 |
| <i>Mave</i> | 3x6 | 0.0 | 0.0 | 1.0 |
| <i>FS</i> | 1x1 | - | - | - |

of ascending neuromodulatory systems in that it is triggered by salient events, influences large regions of the simulated nervous system (see section F. *Synaptic plasticity*), and persists for several cycles [16].

D. Whisker input and lag cells

Whisker input to the neural simulation is provided by transforming each whisker packet into a vector of ‘difference values’ according to:

$$diff_k = [w_{k4}(t) - w_{k3}(t), w_{k3}(t) - w_{k2}(t), w_{k2}(t) - w_{k1}(t), w_{k1}(t) - w_{k4}(t-1)] \quad (5)$$

for whisker w_k at simulation cycle t . These values from the whisker in each column provide input to the corresponding subregions of area *Th*.

Each subregion of area *Th* contains 20 ‘lag’ cells; neuronal units which respond to input with cell-specific time delays (cells with similar properties exist in the visual thalamus of the cat [15]). Each lag cell is characterized by an internal state (s_i^{in}), an output (s_i), and a cell-specific lag parameter set to be $\psi_i = \frac{0.2}{i}$, $i \in \{1, 2, \dots, 20\}$ for cell i in each subregion. When triggered by a whisker deflection, the internal state s_i^{in} of cell i in the corresponding subregion increases at rate determined by the lag parameter ψ_i . When this internal state reaches a threshold, the cell begins to emit an output signal and s_i^{in} is reset to zero. Because of differences in ψ_i among lag cells, each whisker deflection evokes a wave of activity in the corresponding subregion, with some cells firing shortly after deflection and the remainder firing with gradually increasing delays (see Fig. 3, inset).

Specifically, s_i^{in} in the subregion corresponding to whisker w_k , is updated according to:

$$s_{ki}^{in}(t+1) = \begin{cases} 0.2 & s_{ki}^{in}(t) < 0.2, \overline{diff}_k(t) > 3.0 \\ 0 & s_{ki}^{in}(t) \geq \sigma_i^{fire} \\ (1 + \psi_i)(s_{ki}^{in}(t)) & \text{otherwise} \end{cases} \quad (6)$$

where $\overline{diff}_k(t)$ is the average $diff_k(t)$ value (a value exceeding 3.0 signifies a whisker deflection), and σ_i^{fire} is a unit-specific firing threshold (Table II).

The output s_{ki} is calculated using

TABLE III
PROPERTIES OF ANATOMICAL PROJECTIONS IN DARWIN IX¹.

| Projection | Arbor | P | $c_{ij}(0)$ |
|----------------------------|----------|-----|---------------|
| $Th \rightarrow S1$ | []0x0 | 1.0 | 13.0,15.0 |
| $S1 \rightarrow S1(intra)$ | []2x8 | 1.0 | -0.45,-0.6 |
| $S1 \rightarrow S2$ | special | - | 0.25,0.25 |
| $FS \rightarrow Amy$ | non-topo | 1.0 | 5.0,5.0 |
| $Amy \rightarrow M_{ave}$ | non-topo | 1.0 | 40.0,40.0 |
| $FS \rightarrow M_{ave}$ | non-topo | 1.0 | 50.0,50.0 |
| $FS \rightarrow S$ | non-topo | 1.0 | 50.0,50.0 |
| $Amy \rightarrow S$ | non-topo | 1.0 | -50.0,-50.0 |
| $S2 \rightarrow Amy$ | non-topo | 1.0 | 0.0001,0.0003 |

$$s_{ki}(t+1) = \begin{cases} \tanh(10(\omega_i(s_{ki}(t)))) & s_{ki}^{in}(t) < \sigma_i^{fire} \\ \tanh(10(\omega_i(s_{ki}(t))) & \\ +(1 - \omega_i)s_{ki}^{in}(t)) & \text{otherwise} \end{cases} \quad (7)$$

where ω_i determines the persistence of unit activity from one cycle to the next (Table II). This value is fed as input into neuronal units in the corresponding subregions of $S1$.

E. Neuronal dynamics

With the exception of the lag cells in area Th , the state of each neuronal unit in Darwin IX is determined by a mean firing rate variable s , which corresponds to the average activity of a group of roughly 100 real neurons over 100 milliseconds (the ‘output’ of a lag cell (s_{ki}) is equivalent to the mean firing rate of neuronal units in other areas).

The mean firing rate (s) of each neuronal unit ranges from 0 (quiescent) to 1 (maximal firing). For all neuronal units, except those in areas Th and FS , the total contribution of input to unit i is given by

$$A_i(t) = \sum_{l=1}^M \sum_{j=1}^{Nl} c_{ij} s_j(t) \quad (8)$$

where M is the number of different anatomically defined connection types and Nl is the number of connections per type M projecting to unit i (see Table III¹). The activity level of unit i is given by

$$s_i(t+1) = \phi(\tanh(g_i(A_i(t) + \omega s_i(t)))) \quad (9)$$

where $\phi(x) = 0$ for $x < \sigma_i^{fire}$, otherwise $\phi(x) = x$, g_i is a scale factor, and ω determines the persistence of unit activity (Table II).

F. Synaptic plasticity

Synaptic plasticity in Darwin IX acts to strengthen connections between simultaneously active neuronal units in areas $S2$ and Amy . This process is ‘value dependent’, i.e. the degree of

¹Neuronal units connect with a probability (P) and projection shape (Arbor) which can be rectangular “[]” with a height and width (h x w), or non-topographical “non-topo” where all pairs of neuronal units have an equal probability of being connected. The initial connection strengths, $c_{ij}(0)$, are set randomly within the range (min, max). Connections marked with “intra” denote those within a sub-area.

change is modulated by activity in the simulated value system (area S) according to the following rule:

$$\Delta c_{ij}(t+1) = \eta s_j(t) BCM(s_i(t))(V(t) - 0.1) \quad (10)$$

where η is a fixed learning rate ($\eta = 1.4$), $s_i(t)$ and $s_j(t)$ are the activities of the post- and pre-synaptic units respectively and $V(t)$ is the mean activity in area S . The term $(V(t) - 0.1)$ causes depression of plastic connections in the absence of value system activity.

The function $BCM()$ is based on the rule of Bienenstock *et al.* [2] and is implemented as follows ($\rho = 6$, $\theta_1 = \theta_2 = 0.1$, $k_1 = k_2 = 0.45$):

$$BCM(x) = \begin{cases} 0 & x < \theta_1 \\ k_1(\theta_1 - x) & \theta_1 \leq \frac{\theta_1 + \theta_2}{2} \\ k_1(x - \theta_2) & \frac{\theta_1 + \theta_2}{2} \leq x < \theta_2 \\ \frac{k_2 \tanh(\rho(x - \theta_2))}{\rho} & \text{otherwise} \end{cases} \quad (11)$$

G. Aversive conditioning

Synaptic plasticity supports conditioned aversion to texture as follows. Area S maintains a baseline level of activity (0.1) in the absence of input ($\sigma_i^{fire} = -0.1$, see Table II). Detection of a simulated foot-shock (see section H. *Experimental environment and protocol*) causes neuronal units in area FS to produce a steady output of magnitude 1.0. This output pushes activity in area S above baseline, which causes potentiation of synapses onto neuronal units in area Amy from units in $S2$ corresponding to the currently present texture (see equations (10,11)). Freezing/escape responses are triggered by activity in M_{ave} exceeding a threshold (0.5) as a result of input from areas FS and/or Amy (see Fig. 3). This model also supports extinction of conditioned responses: If Amy is activated without any corresponding foot-shock, area S will be inhibited such that its firing rate falls below baseline, and currently active synapses between Amy and $S2$ will be weakened (see equations (10,11)).

H. Experimental environment and protocol

Fig. 4 shows the overall arrangement of Darwin IX’s environment. One texture ($T1$) consists of a vertically aligned column of pegs, the other ($T2$) consists of a vertically staggered set of pegs with offsets of ~ 6 cm (see Fig. 2B). Two adjacent walls contained $T1$, the other two contained $T2$, and either $T1$ or $T2$ can be associated with a simulated aversive foot-shock. Note that Darwin IX typically travels in both clockwise and anticlockwise directions around the environment such that the textures deflect both the left and right whisker arrays. Moreover, in the case of $T2$, the pattern of whisker deflection depends on the direction of travel.

Experiments were divided into training and testing stages. During training, either $T1$ or $T2$ was paired with foot-shock and Darwin IX autonomously explored its enclosure for 25,000 cycles, corresponding to ~ 48 encounters with each wall and ~ 24 aversive responses to the simulated foot-shock. During

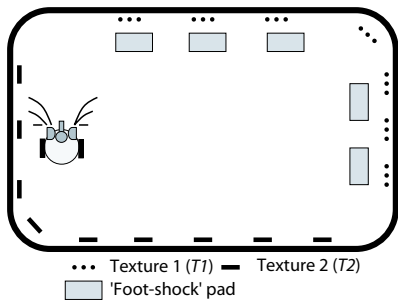


Fig. 4. Experimental setup for Darwin IX. Darwin IX explored a walled enclosure (2.41m x 2.95m) with textures $T1$ and $T2$ on the walls. Instances of each texture were regularly spaced along the walls at intervals of ~ 30 cm. Located on the floor adjacent to $T1$ patterns were ‘foot-shock’ pads made of reflective construction paper. Training and testing was repeated for each Darwin IX subject after exchanging the positions of $T1$ and $T2$.

testing, the foot-shock pads were removed and Darwin IX was allowed to explore its enclosure for 15,000 cycles. Training and testing were repeated using three Darwin IX ‘‘subjects’’ initialized with different random seeds, and pairing both $T1$ and $T2$ with foot-shocks (six training/testing episodes in total). During training and testing of each subject, responses of all neuronal units were recorded and saved for analysis. The position of Darwin IX was also continuously recorded by an overhead camera that detected an array of LEDs positioned on the top surface of the robotic device, the images from which were time-stamped for analysis.

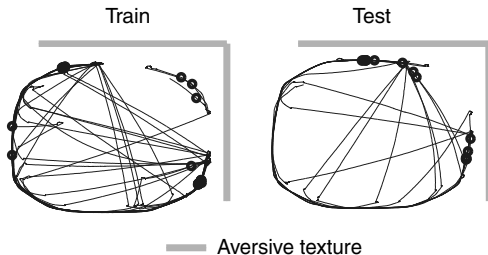


Fig. 5. Conditioned aversion to textures by Darwin IX. The line tracings show the trajectory of a single Darwin IX subject during aversive conditioning to texture $T1$ (left), and during testing (right). Large black dots show locations of aversive responses, gray shading shows locations of $T1$. During testing all freezing/escape responses occurred in proximity to the aversive texture $T1$.

III. RESULTS

Texture discrimination by Darwin IX subjects was assessed by monitoring trajectories during testing. Fig. 5 shows the behavior of a single Darwin IX subject during training in which foot-shock was paired with $T1$, and during testing, in which the foot-shock pads were removed. Most aversive responses were in regions associated with the aversive texture.

Taking into account data from all subjects reveals near perfect conditioned avoidance of aversive textures. During testing, Darwin IX subjects which were trained to avoid $T1$ made aversive responses on 96.6% (S.E. = 0.18%) of encounters with $T1$. When trained to avoid $T2$, these subjects made aversive responses on 97.9% (S.E. = 0.14%) of encounters with $T2$ during testing. Only 3.2% of all aversive responses

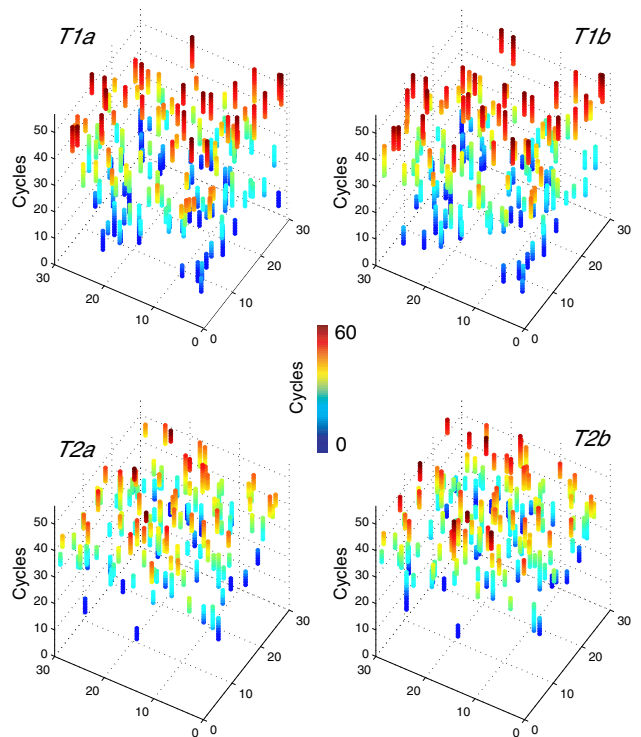


Fig. 6. Spatiotemporal response properties of neuronal units in $S2$. The top panels show $S2$ activity during two separate encounters (a,b) with texture $T1$ by Darwin IX’s left whisker column. The bottom panels show encounters of the same whiskers with texture $T2$. Each panel shows the activity of the 30x30 matrix of $S2$ neuronal units (x and y axes) over 60 post-stimulus cycles (indicated by the z axis as well as by the color scale). Neuronal units are shown if their activity exceeded a threshold (0.25).

during testing occurred inappropriately, i.e. in response to whisker deflections by walls or by the texture not associated with foot-shock.

Darwin IX’s ability to categorize textural stimuli is supported by spatiotemporal patterns of activity in neural area $S2$. Each texture deflects whiskers in a column in a specific temporal order. The lag cells in area Th and neural units downstream in $S1$ (see Fig. 3) present a pattern of activity with both a spatial component (i.e. the particular whisker) and a temporal component (i.e. the time since deflection). $S2$ responds to particular combinations of this $S1$ activity.

The population response of $S2$ to a texture was specific and repeatable. Fig. 6 shows representative $S2$ activity patterns during testing of a Darwin IX subject. The top panels show $S2$ activity during encounters of the left whisker column with texture $T1$. The bottom panels show encounters of the same whiskers with texture $T2$. While all panels show complex spatiotemporal patterns of activity, the top panels are highly similar to each other, the bottom panels are also highly similar to each other, but the top and bottom panels are dissimilar. This observation is supported quantitatively by measures of pattern similarity over time for all possible pairs, calculated as the normalized vector product (see Fig. 7). As shown in this figure, there is high similarity between activity patterns

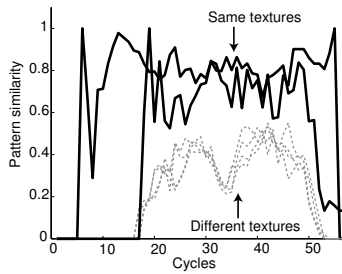


Fig. 7. Similarity over time between pairwise combinations of activity patterns shown in Fig. 5, calculated as $sim(i, j) = v_i(t) \bullet v_j(t)$ where $v_i(t)$ is the normalized neuronal unit activity vector for pattern i at time t . Patterns representing the same texture are highly similar over time (solid black lines; $sim(T1a, T1b)$, $sim(T2a, T2b)$), but patterns representing different textures are not similar (dashed gray lines; $sim(T1a, T2a)$, $sim(T1a, T2b)$, $sim(T2a, T1a)$, $sim(T2a, T1b)$).

representing the same texture, but not between activity patterns representing different textures.

IV. CONCLUSION

Darwin IX categorizes objects based on haptic sensing and learns behavioral responses selective to specific textures. Observations of Darwin IX show that time-lagged neuronal responses to somatosensory input together with value-dependent synaptic plasticity provide a plausible mechanism for the spatiotemporal transformations of sensory input needed for texture discrimination. This mechanism can provide a basis for selective conditioned aversion to textures.

Distinguishing among textures using only the information provided by whiskers involves multiple spatiotemporal transformations. The spatial patterns of textures are transformed, by self-movement, into temporal patterns of whisker deflections, which are themselves transformed into spatiotemporal patterns of neural activity in area $S2$, via a combination of the intrinsic properties of lag cells in area Th and the arrangement of projections in the pathway $Th \rightarrow S1 \rightarrow S2$.

As a result, neuronal units in $S2$ respond to specific combinations of whisker deflections with particular post-stimulus delays. Analysis of neural activity in $S2$ revealed the formation of spatiotemporal activity patterns corresponding to specific haptic perceptual categories (Fig. 6). The response properties of these units are analogous to cells with complex spatiotemporal receptive fields that have been found in rat somatosensory cortex [7] as well as in cat visual cortex [4].

Texture discrimination by Darwin IX was assessed behaviorally by a paradigm based on fear conditioning in which one texture was paired with a simulated foot-shock. In this paradigm, simulated foot-shock triggers a freezing/avoidance response and activates a value system which modulates synaptic plasticity between $S2$ and a neural area analogous to the rodent amygdala (Amy). Activity in Amy evokes a conditioned freezing and avoidance response via excitatory projections to M_{ave} . As a result of these interactions, Darwin IX became conditioned to avoid the aversive texture.

Previous work on whisker-based perception in autonomous robots has focused either on texture discrimination by a fixed

whisker array [6], [10], [14], or on obstacle avoidance by a mobile robot [3], [9]. Darwin IX extends these studies by showing texture discrimination using whisker arrays mounted on a behaving device, and by incorporating a neural simulation based on the rat somatosensory system. Our approach illustrates a very general mechanism for implementing spatiotemporal transformations that may underlie whisker-based perception in a variety of behavioral tasks.

ACKNOWLEDGMENT

This work was supported by the W.M. Keck Foundation and the Neurosciences Research Foundation. We thank J. Snook, D. Hutson, and D. Moore for their contribution to the design of Darwin IX. Address correspondence to Anil K. Seth, seth@nsi.edu.

REFERENCES

- [1] N. Almassy, G.M. Edelman, and O. Sporns. Behavioral constraints in the development of neuronal properties: a cortical model embedded in a real-world device. *Cerebral Cortex*, 8:346–361, 1998.
- [2] E.L. Bienenstock, L.N. Cooper, and P.W. Munro. Theory for the development of neuron selectivity: orientation specificity and binocular interaction in the visual cortex. *Journal of Neuroscience*, 2(1):32–48, 1982.
- [3] R.A. Brooks. A robot that walks: Emergent behaviors from a carefully evolved network. *Neural Computation*, 1:153–162, 1989.
- [4] G.C. DeAngelis, I. Ohzawa, and R.D. Freeman. Receptive-field dynamics in the central visual pathways. *Trends in Neurosciences*, 18(10):451–8, 1995.
- [5] G.M. Edelman, G.N. Reeke, W.E. Gall, G. Tononi, D. Williams, and O. Sporns. Synthetic neural modeling applied to a real-world artifact. *Proc. Nat. Acad. Sci. USA*, 89(15):7267–71, 1992.
- [6] M. Fend, S. Bovet, H. Yokoi, and R. Pfeifer. An active artificial whisker array for texture discrimination. In *Proceedings of the IEEE/RSJ International Conference on Intelligent Robots and Systems (IROS)*, 2003.
- [7] A.A. Ghazanfar and M.A.L. Nicolelis. Spatiotemporal properties of layer V neurons of the rat primary somatosensory cortex. *Cerebral Cortex*, 9:348–361, 1999.
- [8] M.A. Harvey, R. Bermejo, and H.P. Zeigler. Discriminative whisking in the head-fixed rat: optoelectronic monitoring during tactile detection and discrimination tasks. *Somatosens. Mot. Res.*, 18(3):211–22, 2001.
- [9] D. Jung and A. Zelinsky. Whisker-based mobile robot navigation. In *Proceedings of the IEEE/RSJ International Conference on Intelligent Robots and Systems (IROS)*, pages 497–504, 1996.
- [10] M. Kaneko, N. Kanayama, and T. Tsuji. Active antenna for contact sensing. *IEEE Transactions on Robotics and Automation*, 14(2):278–291, 1998.
- [11] J.L. Krichmar and G.M. Edelman. Machine psychology: Autonomous behavior, perceptual categorization and conditioning in a brain-based device. *Cerebral Cortex*, 12(8):818–30, 2002.
- [12] S. Maren and M.S. Fanselow. The amygdala and fear conditioning: has the nut been cracked? *Neuron*, 16(2):237–40, 1996.
- [13] T. Prigg, D. Goldreich, G.E. Carvell, and D.J. Simons. Texture discrimination and unit recordings in the rat whisker/barrel system. *Physiol. Behav.*, 77, 2002.
- [14] R. Russell. Using tactile whiskers to measure surface contours. In *Proc. IEEE International Conference on Robotics and Automation*, pages 1295–1300, 1992.
- [15] A.B. Saul and A.L. Humphrey. Evidence of input from lagged cells in the lateral geniculate nucleus to simple cells in cortical area 17 of the cat. *J. Neurophysiol.*, 68(4):1190–208, 1992.
- [16] W. Schultz, P. Dayan, and P.R. Montague. A neural substrate of prediction and reward. *Science*, 275(5306):1593–9, 1997.